ELSEVIER

Marine Geology 229 (2006) 199–208

MARINE GEOLOGY
INTERNATIONAL JOURNAL OF MARINE GEOLOGY, GEOCHEMISTRY AND GEOPHYSICS

www.elsevier.com/locate/margeo

Anthropogenic Pb component in hydrothermal ochres from Marsili Seamount (Tyrrhenian Sea)

Vesselin M. Dekov [a,*], George D. Kamenov [b], Carlo Savelli [c], Jens Stummeyer [d]

[a] *Department of Geology and Paleontology, University of Sofia, 15 Tzar Osvoboditel Boulevard, 1000 Sofia, Bulgaria*
[b] *Department of Geological Sciences, University of Florida, 241 Willamson Hall, Gainesville, FL 32611, USA*
[c] *Istituto di Geologia Marina, CNR, Via Gobetti 101, 40129 Bologna, Italy*
[d] *Bundesanstalt für Geowissenschaften und Rohstoffe, Stilleweg 2, D-30655 Hannover, Germany*

Received 19 June 2005; received in revised form 26 February 2006; accepted 14 March 2006

Abstract

Recent hydrothermal Fe-oxyhydroxide precipitates (ochres) were sampled during two submersible expeditions to the NE part of the Marsili Seamount summit (SE Tyrrhenian Sea). The Marsili ochres belong to type 1 primary sulfide-poor Fe-oxyhydroxides according to the classification of Hekinian et al. [Hekinian, R., Hoffert, M., Larqué, P., Cheminée, J.L., Stoffers, P., Bideau, D., 1993. Hydrothermal Fe and Si oxyhydroxide deposits from south Pacific intraplate volcanoes and East Pacific Rise axial and off-axial regions. Econ. Geol. 88, 2099–2121]. They are X-ray amorphous, highly metalliferous [Al/(Al+Mn+Fe) ≪ 0.4], low in Si, transition metals (Co, Ni, Cu, Zn, Pb) and rare earth elements (REE) and enriched in B, V and Mo. Their chemical composition and REE distribution patterns indicate precipitation from low-temperature hydrothermal fluid mixed with seawater. Measured Pb isotope compositions in the ochres indicate that the Pb is dominantly anthropogenic in origin. By contrast, the Pb isotope ratios in the nearby higher temperature hydrothermal deposits from the Panarea arc volcano show that the Pb is derived mainly from local volcanic rocks. The fact that the Pb isotopic signature of the Marsili ochres is controlled by recent anthropogenic input suggests that the Fe-oxyhydroxides precipitated from fluids depleted in transition metals. The low $^{206}Pb/^{207}Pb$ ratios in the ochres reflect the contribution of Pb from Australian ores, indicating precipitation of the ochres somewhere between present-day and the beginning of Australian Pb import to Europe. The young age of the ochres and the presence of other hydrothermal deposits along the Marsili crest suggest that the magmatic chamber beneath the seamount may still be alive. This study represents the first observation of anthropogenic influence on submarine hydrothermal deposits.
© 2006 Elsevier B.V. All rights reserved.

Keywords: hydrothermal ochres; anthropogenic Pb; Marsili Seamount; Tyrrhenian Sea

1. Introduction

Submarine hydrothermal activity and deposits in the Tyrrhenian Sea have been studied since the late 1960s (Dekov and Savelli, 2004 and references therein). Research has focused primarily on the oxyhydroxide and sulfide occurrences of the Eolian volcanic ring in the Marsili Basin (SE Tyrrhenian Sea). Among the earlier reports on hydrothermal occurrences at Marsili Seamount (Rozanova et al., 1988; Sborshchikov et al., 1988; Uchupi and Ballard, 1989; Marani et al., 1999) none contain descriptions of the composition and origin of these deposits.

* Corresponding author. Tel.: +359 2 9308 276; fax: +359 2 446 487.
E-mail address: dekov@gea.uni-sofia.bg (V.M. Dekov).

0025-3227/$ - see front matter © 2006 Elsevier B.V. All rights reserved.
doi:10.1016/j.margeo.2006.03.003

In this paper, we present data and discuss the origin of Fe-ochres sampled during submersible surveys at the crest of the Marsili Seamount.

2. Geological setting

Marsili Basin is an active back-arc basin floored by oceanic crust, encircled by a volcanic arc and fore-arc system. These features overlie the northwest dipping Ionian subduction zone (Argnani and Savelli, 1999) (Fig. 1A). The Marsili abyssal plain (~3500 m deep) occupies the central part of the basin. Marsili Seamount is a <0.8 Ma old back-arc spreading centre (Savelli and Gasparotto, 1994) and rises ~3000 m from the even abyssal plain. It is a large (~60×30 km) volcanic seamount trending approximately N–S (Fig. 1A,B) with a narrow crest and numerous cones on the flanks (Marani et al., 1999, 2004). Dredge hauls and submersible dives (Sborshchikov et al., 1988; Marani et al., 1999) revealed that the summit area was covered by fresh pillow and ropy lava flows. High heat flow has been measured at the seamount crest (Rozanova et al., 1988). A remote TV survey and submersible observations revealed an extensive area of hydrothermal deposition on the shallowest peak (~500 m deep) at the NE end of Marsili Seamount (Sborshchikov et al., 1988; Uchupi and Ballard, 1989). This area was sampled by submersibles. At the sampling sites, the basalts exhibit orange-red and yellow to white features related to hydrothermal alteration. The seafloor is bare of sediment except for thin (<10 cm) sediment coatings in pockets between pillows.

3. Material and methods

We studied 2 ochre samples taken from among the hydrothermally altered basalts of the Marsili Seamount

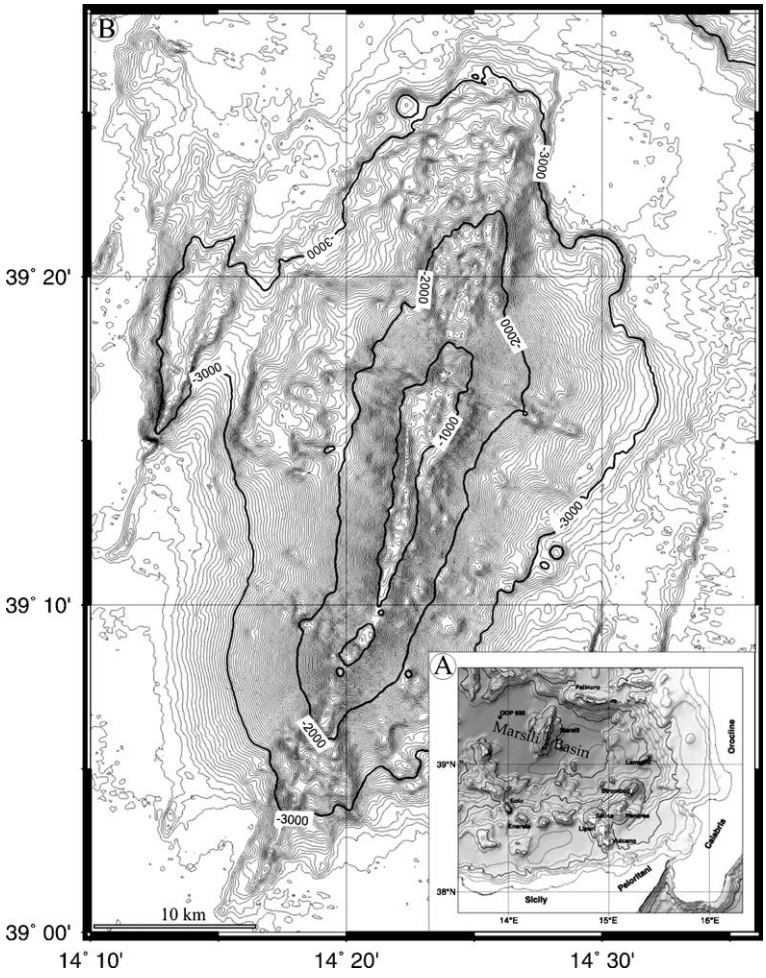


Fig. 1. (A) Generalized map of the Marsili Basin in SE Tyrrhenian Sea; (B) bathymetric map of the Marsili Seamount (contour interval 25 m; after Marani et al., 2004) with sample location (star).

crest (Fig. 1B) during (1) the 18th cruise of the Russian R/V *Vityaz* with the submersible *Argus* (sample Argus 18-467-3, 39°17′N, 14°24′E, 503 m water depth) in 1986, and (2) the 16th cruise of the Russian R/V *Academic M. Keldysh* with the submersibles *MIR-1 and -2* (site 2012, sample MIR-2-5/16-4/3, 39°17′N, 14°24′ E, 520 m water depth) in 1988.

Whole-rock mineralogy was determined by X-ray diffraction (XRD): Philips X-ray diffractometer PW 1710 with monochromatic Co K_α radiation, 40 kV, 30 mA; X-ray scans from 2 to 88°2θ, with step 0.04°2θ, and velocity 1.5 s/step. Scanning electron microscope (SEM) observations were made on Au-coated fragments of bulk samples using a JEOL JSM-5410LV electron microscope coupled with EDS.

The chemical composition of the samples was determined by X-ray fluorescence spectrometry (XRF) and Inductively Coupled Plasma Mass Spectrometry (ICP-MS). XRF analyses were performed using Philips PW 2400 and PW 1480 wavelength dispersive spectrometers. Forty-two major and trace elements were analysed quantitatively after fusion of 1 g sample material with 5 g lithium metaborate at 1200 °C for 20 min. Quality of the results was controlled with certified reference materials from BCR (Community Bureau of Reference, Brussels). This procedure ensured an analytical precision better than ±0.5% for major elements and 1–10 ppm for trace elements (analytical precision for XRF analyses of certified reference materials). Trace elements and Rare Earth Elements (REE) were analysed by ICP-MS (Perkin Elemer Sciex Elan 5000) after wet chemical decomposition of the samples in a closed microwave system (3 ml HF, 1 ml HNO_3 suprapure quality, 0.5 g sample). After decomposition, the solutions were treated with $HClO_4$ to remove HF. The quality of the results was controlled using CRM (e.g., NIST CRM 1643d). An analytical precision of ±5% was achieved for major and trace elements.

Marsili ochres and 2 hydrothermal samples from Panarea Island (Aeolian Arc) were dissolved in HF-HNO_3 mixture and Pb was separated in HBr medium using standard chromatographic techniques. Pb isotope analyses were conducted on a Nu-Plasma multi collector ICP-MS (Nu Instruments, UK) using the Tl normalization technique (Kamenov et al., 2004, 2005). The reported Pb isotopic compositions are relative to the following NBS 981 values: $^{206}Pb/^{204}Pb = 16.937$ (±0.004, 2SE), $^{207}Pb/^{204}Pb = 15.491$ (±0.004, 2SE), $^{208}Pb/^{204}Pb = 36.695$ (±0.009, 2SE), $^{207}Pb/^{206}Pb = 0.91459$ (±0.00007, 2SE), and $^{208}Pb/^{206}Pb = 2.1665$ (±0.0002, 2SE).

4. Results

4.1. Mineralogy, geochemistry, and classification

The studied ochres were yellow-brown with an earthy appearance and massive (unlayered) texture. XRD investigations indicate that the ochres are X-ray amorphous. SEM-EDS studies reveal that the ochres are composed of Fe-Si-oxide colloform masses, which exhibit features of incipient crystallization, the very earliest stage of X-ray amorphous Fe-oxyhydroxide ordering (Fig. 2).

The chemical composition of the investigated ochres resembles that of similar Fe-oxyhydroxide deposits from the off-axial seamounts [Red Seamount at 21°N East Pacific Rise (EPR), Seamount 5 at 13°N EPR], back-arc (Kameni Islands, Santorini) and arc (Tutum Bay, Ambitle Island, SW Pacific Ocean) volcanoes, and back-arc spreading centers (Franklin Seamount, Woodlark Basin) (Table 1). The Marsili ochres are highly metalliferous [Al/(Al+Mn+Fe)<0.4] (Bonatti, 1981). Their bulk composition is characterized by high Fe (25–50%) and low Si (4–10%) contents (Si/Fe<0.3). The ochres are depleted in transition metals (Co+Ni+Cu+Zn<200 ppm). In the Si–Fe–(Co+Ni+Cu+Zn)×10 triangular diagram (Hekinian et al., 1993), they fall near the Fe-rich corner on the Si–Fe side. The Marsili ochres display higher Mn contents (Mn>1%) compared to the other similar deposits, but their Mn/Fe ratio (0.1) is low (Table 1). They plot near the Fe apex of the Mn–Fe–(Co+Ni+Cu)×10 ternary diagram of Bonatti et al. (1972), consistent with a hydrothermal origin. Trace metals that form stronger hydroxy complexes in water

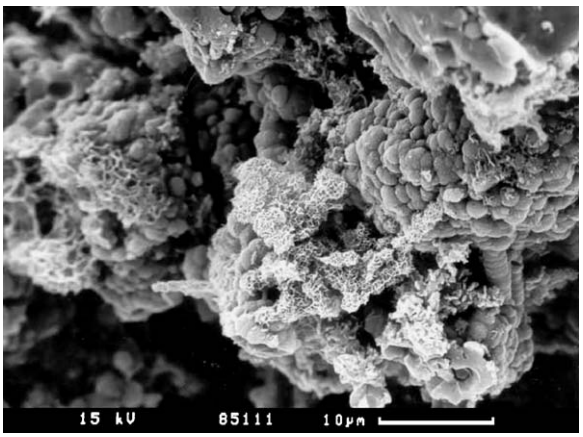


Fig. 2. SEM microphotograph of an ochre sample (secondary electron image; sample Argus 18-467-3): Fe–Si colloform mass at stage of incipient crystallization [note the small (<1 μm) blade-like crystals].

Table 1
Chemical composition of investigated ochres from Marsili Seamount and elsewhere

Element	Argus 18-467-3	MIR-2-5/ 16-4/3	Average Tyrrhenian metalliferous sediment[a]	21°N EPR, Red Smt, 1642-KA[b]	13°N EPR, Smt 5, 1400-PC1A[b]	Kameni Islands, Santorini, Fe-muds[c]	Tutum Bay, Ambitle Island, Fe-oxyhydroxides[d]	Franklin Smt, Woodlark Basin, Fe-oxyhydroxide deposits[e]
Si, %	7.55	3.53	18	6.25	9.78	8.69	7.19	10.5
Al	0.83	0.20	4	0.14	0.12	0.40	<0.1	0.36
Ti	0.04	0.01	0.28	0.02	0.03	0.09	<0.01	0.09
Fe	31.3	36.2	14	24.8	20.5	23.3	29.9	41.8
Mn	3.28	4.17	5.9	0.09	0.14	0.05	0.06	0.95
Mg	0.67	1.11	2.1	0.52	0.45	0.83	0.56	0.59
Ca	0.82	1.09	8.1	0.62	0.62	1.15	1.95	0.99
Na	1.91	1.39	1.3	0.34	0.34	1.91	0.29	2.11
K	0.78	0.43	1.1	0.13	0.15	–	0.07	0.37
P	0.48	0.34	0.15	0.81	0.56	0.18	0.05	0.89
LOI	25.1	25.9	–	8.70	14.9	–	19.8	–
Al/(Al+Fe+Mn)	0.023	0.005	0.17	0.005	0.006	0.017	0.003	0.008
Mn/Fe	0.10	0.11	3.2	0.004	0.007	0.002	0.002	0.023
Si/Fe	0.24	0.10	1.29	0.25	0.48	0.37	0.24	0.25
Ag, ppm	0.05	0.02	–	–	–	–	1.21	3.0
B	164	192	–	–	–	–	–	–
Ba	194	306	641	200	210	77	127	1110
Be	1.8	7.0	–	–	–	–	38	0.6
Bi	0.06	0.01	–	–	–	0.05	–	–
Cd	0.32	0.35	–	–	–	–	–	1.0
Co	12.9	2.4	125	10	26	–	<5	46
Cr	9.2	16.7	165	11	14	–	28.6	29
Cs	1.9	0.2	–	0.4	–	–	2.4	4.9
Cu	68.3	12.9	91	50	4	15	51.6	39
Ga	2.6	1.5	–	–	–	–	1.4	2.3
Ge	17.5	20.7	–	–	–	–	–	10.6
Hf	0.4	0.2	–	0.18	–	–	<0.05	0.54
In	0.01	0.01	–	–	–	–	0.07	–
Li	8.9	10.7	–	–	–	–	–	47.2
Mo	182	183	135	–	–	–	1.4	232
Nb	1.6	0.2	16	–	–	–	<10	–
Ni	22.1	34.9	177	<90	10	15	0.25	196
Pb	17.8	4.4	54	20	30	–	22.9	19
Rb	12.3	2.0	231	<50	<10	–	6.7	63
Sb	6.9	13.5	–	1.3	<3	1.67	212	6.7
Sc	1.6	0.7	27	0.79	–	–	–	1.9
Sn	9.1	0.1	–	–	–	–	–	–
Sr	244	435	842	350	110	86	725	480
Ta	0.18	0.08	–	0.07	–	–	159	–
Th	1.12	0.14	16	0.36	6	–	–	0.2
Tl	5.8	13.8	–	–	–	–	2.07	8.9
U	5.3	33.5	–	14.5	8	–	0.65	5.3
V	300	477	198	–	–	111	33	270
W	1.51	4.17	–	–	–	–	<10	3.5
Y	13.8	19.5	28	–	–	30	15.1	12.1
Zn	58	47	170	20	14	63	57	45
Zr	30	18	114	–	–	46	2.1	8.2
La	9.5	5.2	22	2.9	–	–	5.3	3.3
Ce	13.2	7.8	42	4.1	–	–	7.2	4.1
Pr	1.76	1.18	4.5	–	–	–	0.95	0.7
Nd	7.15	5.34	17	–	–	–	4.73	3.5
Sm	1.45	1.35	3.5	0.41	–	–	1.14	0.96
Eu	0.34	0.29	0.72	0.09	–	–	0.46	0.48
Gd	1.78	2.11	3.4	–	–	–	1.81	1.4
Tb	0.26	0.37	0.54	0.07	–	–	0.26	0.36

Table 1 (*continued*)

Element	Argus 18-467-3	MIR-2-5/ 16-4/3	Average Tyrrhenian metalliferous sediment[a]	21°N EPR, Red Smt, 1642-KA[b]	13°N EPR, Smt 5, 1400-PC1A[b]	Kameni Islands, Santorini, Fe-muds[c]	Tutum Bay, Ambitle Island, Fe-oxyhydroxides[d]	Franklin Smt, Woodlark Basin, Fe-oxyhydroxide deposits[e]
Dy	1.64	2.80	3.0	–	–	–	1.52	1.4
Ho	0.37	0.68	0.82	–	–	–	0.31	0.31
Er	1.05	2.12	2.0	–	–	–	0.77	1.05
Tm	0.15	0.32	0.31	–	–	–	0.11	0.06
Yb	0.90	2.07	1.9	0.41	–	–	0.54	0.96
Lu	0.16	0.37	0.34	0.13	–	–	0.07	0.1
ΣREE	39.7	32.0	102	–	–	–	25.1	18.7
(Ce/Ce^*)[f]	0.73	0.75	0.92	–	–	–	0.72	0.63
(Eu/Eu^*_1)[g]	0.65	0.52	1.00	–	–	–	0.97	1.26
(Eu/Eu^*_2)[h]	0.71	0.53	0.67	0.70	–	–	1.1	1.0
La_N/Lu_N	6.38	1.49	0.74	2.47	–	–	8.1	3.5
Cs/Sb	0.27	0.01	–	0.31	–	–	0.01	0.73
Cs/Tl	0.33	0.01	–	–	–	–	1.16	0.55
Rb/Sb	1.78	0.15	–	–	–	–	0.03	9.40
Rb/Tl	2.12	0.14	–	–	–	–	3.24	7.08

[a] Dekov and Savelli (2004).
[b] Alt (1988).
[c] Mean from 72 analyses: Puchelt (1973); Puchelt et al. (1973); Boström and Widenfalk (1984); Varnavas and Cronan (1988).
[d] Mean from 16 analyses: Pichler and Veizer (1999).
[e] Mean from 66 analyses: Bogdanov et al. (1997).
[f] $Ce/Ce^* = 2Ce_N/(La_N + Pr_N)$.
[g] $Eu/Eu^*_1 = 2Eu_N/(Sm_N + Gd_N)$.
[h] $Eu/Eu^*_2 = 2Eu_N/(Sm_N + Tb_N)$.

(Sb, Tl) are enriched in the Marsili ochres compared to other elements that form weaker complexes (Rb, Cs) (e.g., Pichler and Veizer, 1999). Thus, the Cs/Sb, Cs/Tl, Rb/Sb and Rb/Tl ratios are generally very low (Table 1). The ochres are enriched in elements that have a strong affinity for Fe such as B, V, and Mo. Marsili ochres are depleted in REE (ΣREE<40 ppm). Their REE distribution patterns show small negative Ce and Eu anomalies and relative enrichment of LREE compared to HREE (Fig. 3, Table 1).

Hekinian et al. (1993) classified hydrothermal Fe- and Si-oxyhydroxide deposits into four types based on their geologic setting, morphology and composition. According to this classification, the ochres studied here are type 1 deposits: primary Fe-oxyhydroxides forming chimneys, mounds and flat-lying deposits.

4.2. Pb isotopes

Measured Pb isotopes in Marsili ochres and altered basalt, and Panarea sulfides are presented in Table 2. A sample of altered basalt from Site 2012 shows relatively high Pb isotope ratios with $^{206}Pb/^{204}Pb = 19.228$, $^{207}Pb/^{204}Pb = 15.673$ and $^{208}Pb/^{204}Pb = 39.151$. These ratios are indistinguishable from those of fresh basalt samples from the Marsili Seamount (Dekov et al., submitted for publication). The two ochre samples have $^{206}Pb/^{204}Pb = 18.401$ and 18.235, $^{207}Pb/^{204}Pb = 15.649$ and 15.635, and $^{208}Pb/^{204}Pb = 38.446$ and 38.367, ratios that are much lower compared to fresh and altered Marsili Seamount basalts. The two Panarea sulfides have similar Pb isotopic compositions with $^{206}Pb/^{204}Pb = 19.094$ and 19.081, $^{207}Pb/^{204}Pb = 15.689$ and $^{208}Pb/^{204}Pb = 39.130$ and 39.118, distinct from the Marsili ochre samples.

5. Discussion

5.1. Geochemistry of the ochres

The REE patterns for the Marsili ochres are similar to that of seawater (excluding the levels of Ce anomaly) and comparable to the REE distribution patterns of other low-temperature Fe-oxyhydroxide deposits (Fig. 3; Hekinian et al., 1993). The negative Ce anomaly is typical of low-temperature submarine hydrothermal deposits (Marchig et al., 1982; Glasby et al., 1997) and rapidly growing sub-oxic diagenetic nodules (Reyss et al., 1985). However, the low total REE abundance, trace metal and Mn contents reflect a low-temperature hydrothermal rather than sub-oxic diagenetic origin for the ochres. The negative Ce anomaly is less than that of deep seawater and can be attributed to the mixing of

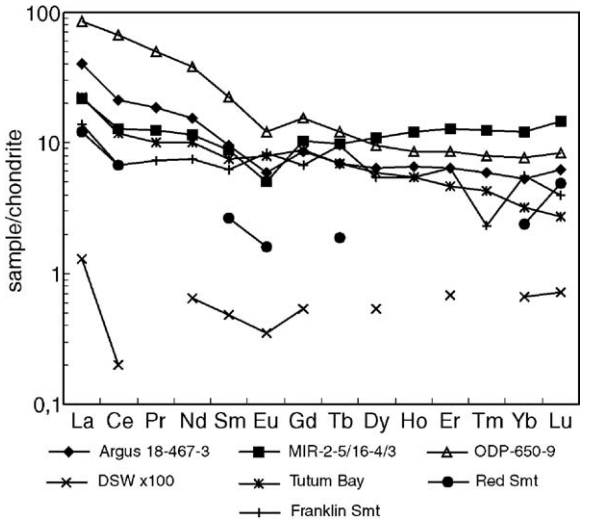


Fig. 3. C1 chondrite-normalised (Sun and McDonough, 1989) REE distribution patterns for the Marsili ochres (Argus 18-467-3, MIR-2-5/16-4/3), Tyrrhenian pelagic calcareous oozes (ODP Site 650, sample 107-650A-65X-1 (50–53)), western Mediterranean deep seawater (DSW, sample 10708–2750 m; Greaves et al., 1991), Tutum Bay Fe oxyhydroxide deposits (mean from 7 analyses; Pichler and Veizer, 1999), Red Seamount at 21°N EPR (sample 1642-KA; Alt, 1988), Franklin Seamount Fe-oxyhydroxide deposits (mean from 34 analyses; Bogdanov et al., 1997).

seawater with hydrothermal fluids, which exhibit no Ce anomaly (Michard, 1989). The positive Gd anomalies (Fig. 3) are also a seawater signal (de Baar et al., 1985) reflecting western Mediterranean deep seawater. This implies that the observed negative Eu anomalies may not be quite as large as they appear. For this reason, we recalculated the size of Eu anomaly bypassing Gd (Table 1). Despite this maneuver, the Eu anomaly remained almost the same. The negative Eu anomalies suggest that the parent solution from which the ochres precipitated had temperatures <250 °C upon discharge (Michard, 1989). The negative Eu anomaly of the ochres reflects either that in seawater or Eu depletion in the original hydrothermal fluid. There are three possible explanations of such Eu depletion (Hein et al., 2000): (1) hydrothermal minerals with positive Eu anomalies such as barite and anhydrite have precipitated deeper in the system; (2) Eu depletion in the basement rocks leached by the hydrothermal fluids due to previous alteration; and/or (3) no leaching of plagioclase by hydrothermal fluids.

Very low REE/Fe ratios indicate rapid precipitation of the Fe-oxyhydroxides (e.g., Olivarez and Owen, 1989). Rapid precipitation is supported by the X-ray amorphous nature of the Fe-oxyhydroxides (e.g., Hekinian et al., 1993). In addition, the presence of silica probably suppressed Fe-oxyhydroxide crystallization (Schwertmann and Fischer, 1973).

The extremely low transition metal and REE concentrations of the ochres as well as their REE patterns rule out a diagenetic or hydrogenetic origin of the samples. The negative Eu anomalies also exclude a high-temperature hydrothermal origin. The mineralogical and geochemical data suggest that the Marsili ochres precipitated directly from low-temperature hydrothermal fluids following sub-seafloor mixing of ascending hydrothermal fluids with seawater (e.g., Sedwick et al., 1992; Pichler and Veizer, 1999).

5.2. Pb isotope variations

Pb isotope data can be used to indicate possible sources of metals to the Marsili ochres. Fig. 4 shows the Pb isotopic compositions of the studied ochres in comparison with possible sources in the region, which include Marsili lavas and sediments, Saharan dust, sulfide precipitates from Panarea and anthropogenic components. The Marsili ochres display isotopic compositions distinct from the underlying volcanic rocks, Saharan dust, and regional marine sediments, indicating that the Pb is not controlled by natural sources. The Pb isotopic compositions of the ochres plot entirely in the anthropogenic Pb field on Fig. 4 indicating that the Pb is derived from anthropogenic sources. These isotopic compositions also display on a linear trend with the 3 Italian aerosol samples, which suggests possible mixing between natural Pb, either from the basaltic basement and/or sediments and/or Saharan dust, and anthropogenic Pb. There are no data for the Pb isotopic compositions of hydrothermal fluids in the region. However, the sulfide samples from the nearby active Panarea hydrothermal area can be used as

Table 2
Isotopic compositions of samples from the study area

Sample no.	Type	$^{206}Pb/^{204}Pb$	$^{207}Pb/^{204}Pb$	$^{208}Pb/^{204}Pb$
site 2012	Marsili altered basalt	19.228	15.673	39.151
B49	Panarea sulfide[a]	19.094	15.689	39.130
B48	Panarea sulfide[a]	19.081	15.689	39.118
MIR-2-5/16-4/3	Marsili ochre	18.401	15.649	38.446
Argus 18-467-3	Marsili ochre	18.235	15.635	38.367

[a] Described in detail in Marani et al. (1997).

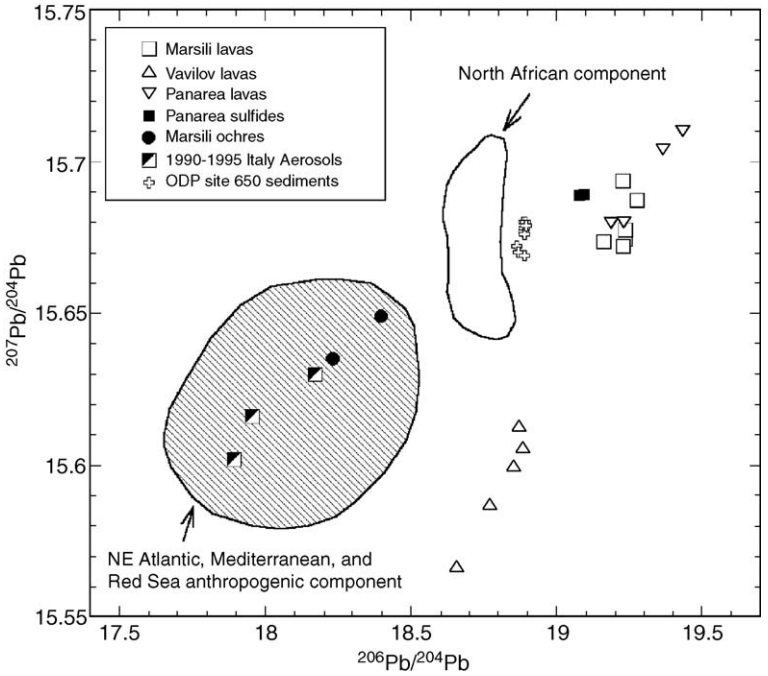


Fig. 4. Comparison of Pb isotopic compositions of Marsili ochres with possible sources in the region, including pre-anthropogenic sediments (ODP site 650), North African material (Saharan dust and North Africa granitoids), Marsilli, Panarea, and Vavilov (Vavilov Basin, W Tyrrhenian Sea) lavas, Panarea sulfides, anthropogenic Pb background, and aerosols sampled over Italy in 1990–1995. Note that the Pb isotopic compositions of the ochres are indistinguishable from the anthropogenic Pb background and distinct from the pre-antropogenic Pb background recorded in ODP site 650 sediments. Data sources: ODP site 650 sediments from Dekov et al. (submitted for publication), Panarea lavas from Calanchi et al. (2002), North Africa granitoids from Juteau et al. (1986), Saharan dust and anthropogenic Pb from Hamelin et al. (1989), Vavilov lavas from Hamelin et al. (1979), Italy aerosols from Tommasini et al. (2000).

an approximate end-member for a hydrothermal contribution.

The Pb isotopic composition of Panarea sulfides is similar to the underlying Panarea lavas and to the Marsilli Seamount lavas (Fig. 4) indicating that the Pb was mainly derived from local volcanic rocks. The isotope data for the mineralization are slightly offset to lower $^{206}Pb/^{204}Pb$ ratios that may indicate minor incorporation of Pb from the local sediments. Alternatively, the Pb isotopic variability in the Panarea volcanic rocks may not be completely represented by the few data points on Fig. 4. Therefore, an alternative explanation for the observed small isotopic difference between Panarea lavas and mineralization can be that the offset reflects derivation of ore Pb from a deeper volcanic unit, as was observed in hydrothermal mineralizations in SW Pacific (Kamenov et al., 2005). Regardless of the nature of the small offset, the overall isotopic similarity between the Panarea mineralization and the local volcanic rocks indicate that Pb and other metals were mainly derived from the latter.

Contrary to Panarea, the Pb isotopic compositions of the Marsili ochres do not indicate derivation of ore metals from local non-anthropogenic sources. Even if we assume mixing relationships for the origin of the Pb in the ochres, the non-anthropogenic component will be relatively small. For example, if the Pb isotopic compositions of Panarea sulfides is used as an approximate measure of the isotopic composition of hydrothermal fluids emanating from the volcanic basement, then mixing calculations between Panarea sulfides and average anthropogenic Pb show a mixture of approximately 20–30% hydrothermal Pb with 70–80% anthropogenic Pb in the Marsili ochres. However, this statement must be treated with caution because the ochres plot entirely within the anthropogenic Pb field. Their Pb isotopic composition, therefore, may be controlled entirely by recent anthropogenic input.

The presence of anthropogenic Pb with relatively low $^{206}Pb/^{207}Pb$ indicates a very young age for the Marsili ochres, anywhere from present-day to around 150 years ago. Shift towards lower $^{206}Pb/^{207}Pb$ ratios in the Pb background in Europe began around 3000 years ago with the onset of Pb mining and smelting (Fig. 5; Shotyk et al., 1998). Between 3000 BP and around 1850 AD the anthropogenic Pb was derived from local sources, and

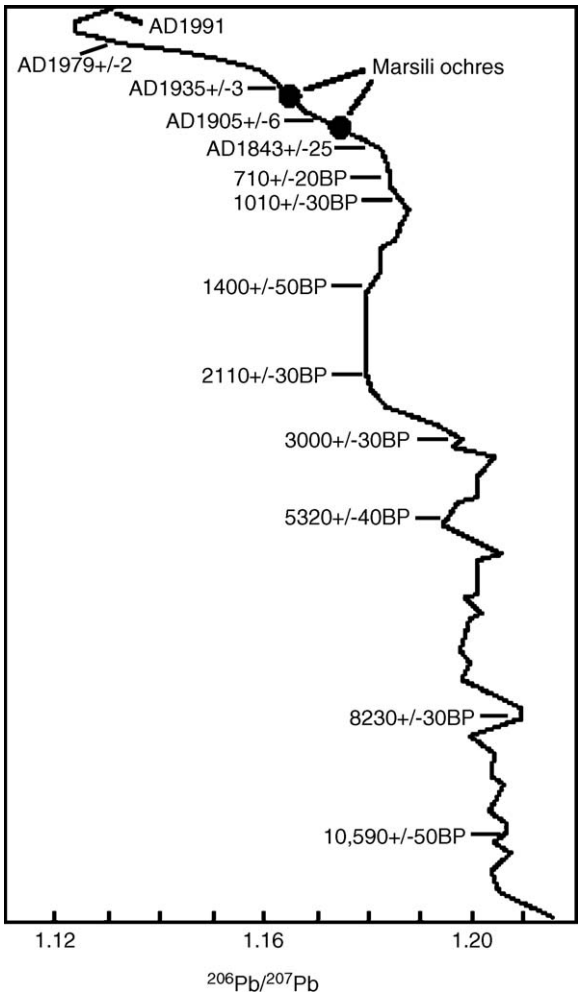


Fig. 5. $^{206}Pb/^{207}Pb$ compositions of Marsili ochres relative to changes in $^{206}Pb/^{207}Pb$ during the last 12,000 years. Pb isotopic curve modified after Shotyk et al. (1998). Pre-antropogenic $^{206}Pb/^{207}Pb$ values cluster around 1.2 then, around 3000 BP Pb mining begins in Europe, which results in slight decrease in $^{206}Pb/^{207}Pb$ values. Sharp decrease in $^{206}Pb/^{207}Pb$ begins after the onset of the industrial revolution with Australian Pb imports. Marsili ochres plot at lower $^{206}Pb/^{207}Pb$ values than the Pb mined in Europe, indicating incorporation of Australian Pb. Based on the position of the ochres on the Pb isotope curve we can conclude that they precipitated within the last 150 years, after the beginning of Australian Pb imports to Europe.

related $^{206}Pb/^{207}Pb$ isotope ratios show slightly lower values compared to the pre-anthropogenic background (Fig. 5; Shotyk et al., 1998). At around 1850 AD the Pb isotopic curve begins a trend towards much lower $^{206}Pb/^{207}Pb$ ratios, with very sharp decline during the 20th century, which is a result of importation of Australian lead to Europe (Fig. 5; Shotyk et al., 1998). The measured $^{206}Pb/^{207}Pb$ ratios in the Marsilli ochres, 1.166–1.176, are lower than the pre-Australian anthropogenic Pb ratios (~1.18) (Fig. 5), indicating that the ochres were precipitated after the beginning of the Pb imports from Australia. The position of the ochres on the Pb curve may be interpreted that the ochres were precipitated somewhere between AD 1843 and AD 1936 (Fig. 5). However, we can not completely rule out mixing relationships as discussed above, therefore, we can state that this age estimate is approximate and the ochres may have formed anywhere between present day and introduction of Australian Pb to Europe.

The Pb isotope ratios for the ochres indicates minor, if any, hydrothermal input of Pb from volcanic rocks. Compared to Panarea sulfides, which inherited their isotopic signature from local volcanic rocks, the Pb in the Marsilli ochres was mainly derived from anthropogenic sources. This indicates that the sulfide component was removed from these low-temperature hydrothermal solutions and the hydrothermal solutions precipitated mainly oxyhydroxides with low concentrations of ore metals.

6. Conclusions

The Marsili ochres resemble other Fe-oxyhydroxide deposits from different tectonic settings in the world ocean: off-axial seamounts at divergent plate margins, back-arc spreading centers and arc settings. According to the classification of Hekinian et al. (1993) the Marsili ochres belong to the type 1 deposits: primary Fe-oxyhydroxides. They are highly metalliferous, depleted in transition metals and REE, and enriched in B, V and Mo. Their REE patterns show small negative Ce and Eu anomalies and relative enrichment of LREE compared to HREE. Marsili ochres are recent deposits, rapidly precipitated from low-temperature hydrothermal solutions. The Pb isotope signature of the ochres suggests that most, if not all of the Pb is derived from modern anthropogenic sources. This anthropogenic influence allows us to conclude that these ochres were formed within the last 150 years, anywhere between present day and the beginning of Australian Pb import to Europe. In contrast, the Pb isotope signature of the nearby Panarea hydrothermal mineralization indicates a Pb source in the local volcanic rocks. The low-temperature Marsili ochres were precipitated from fluids strongly depleted in transitional metals. This is also reflected in the fact that their Pb isotopic composition is swamped by recent anthropogenic input. The young age of the Marsili ochres and the presence of additional Fe-Mn-oxyhydroxide and sulfide occurrences along the Marsili crest (Marani et al., 2004) suggest that the magmatic chamber beneath the seamount is still active.

Acknowledgements

V.M. Dekov gratefully acknowledges the award of a CNR-NATO Senior Fellowship (no. 217.36 S, 12/05/2004-N.5). We are indebted to the pilots of the *Argus, MIR-1 and -2* submersibles for their help in collecting the samples, to M. Marani (ISMAR-CNR, Italy) for supplying the multi-beam bathymetric map of the Marsili Seamount and J.R. Hein (USGS) and T. Pichler (University of South Florida) for their valuable advice. Comments by G.J. De Lange, G.P. Glasby and R. Koski improved the presentation of this material.

References

Alt, J.C., 1988. Hydrothermal oxide and nontronite deposits on seamounts in the eastern Pacific. Mar. Geol. 81, 227–239.

Argnani, A., Savelli, C., 1999. Cenozoic volcanism and tectonics in the southern Tyrrhenian sea: space–time distribution and geodynamic significance. J. Geodyn. 27, 409–432.

Bogdanov, Yu.A., Lisitzin, A.P., Binns, R.A., Gorshkov, A.I., Gurvich, E.G., Dritz, V.A., Dubinina, G.A., Bogdanova, O.Yu., Sivkov, A.V., Kuptsov, V.M., 1997. Low-temperature hydrothermal deposits of Franklin Seamount, Woodlark Basin, Papua New Guinea. Mar. Geol. 142, 99–117.

Bonatti, E., 1981. Metal deposits in the oceanic lithosphere. In: Emiliani, C. (Ed.), The Sea, vol. 7. John Willey and Sons, N.Y., pp. 639–686.

Bonatti, E., Kraemer, T., Rydell, H., 1972. Classification and genesis of submarine iron-manganese deposits. In: Horn, D.R. (Ed.), Ferromanganese Deposits of the Ocean Floor. Arden House, Harriman, NY, USA, pp. 149–165.

Boström, K., Widenfalk, L., 1984. The origin of iron-rich muds at the Kameni Islands, Santorini, Greece. Chem. Geol. 42, 203–218.

Calanchi, N., Peccerillo, A., Tranne, C.A., Lucchini, F., Rossi, P.L., Kempton, P., Barbieri, M., Wu, T.W., 2002. Petrology and geochemistry of volcanic rocks from the island of Panarea: implications for mantle evolution beneath the Aeolian Island Arc (southern Tyrrhenian Sea). J. Volcanol. Geotherm. Res. 115, 367–395.

de Baar, H.J.W., Brewer, P.G., Bacon, M.P., 1985. Anomalies in rare earth distributions in seawater: Gd and Tb. Geochim. Cosmochim. Acta 49, 1961–1969.

Dekov, V.M., Savelli, C., 2004. Hydrothermal activity in the SE Tyrrhenian Sea: an overview of 30 years of research. Mar. Geol. 204, 161–185.

Dekov, V.M., Kamenov, G., Savelli, C., Stummeyer, J., Marchig, V., submitted for publication. Origin of basal dolomitic claystone in the Marsili Basin (Tyrrhenian Sea): hydrothermal metasomatism or seawater convection through the calcareous−eolian sediment. Mar. Geol.

Glasby, G.P., Stüben, D., Jeschke, G., Garbe-Schönberg, C.-D., 1997. A model for the formation of hydrothermal manganese crusts from the Pitcairn Island hotspot. Geochim. Cosmochim. Acta 61, 4583–4597.

Greaves, M.J., Rudnicki, M., Elderfield, H., 1991. Rare earth elements in the Mediterranean Sea and mixing in the Mediterranean outflow. Earth Planet. Sci. Lett. 103, 169–181.

Hamelin, B., Lambret, B., Joron, J., Treuil, M., Allegre, C.J., 1979. Geochemistry of basalts from the Tyrrhenian Sea. Nature 278, 832–834.

Hamelin, B., Grousset, F.E., Biscaye, P.E., Zindler, A., 1989. Lead isotopes in Trade Wind aerosols at Barbados: the influence of European emissions over the North Atlantic. J. Geophys. Res. 94, 16243–16250.

Hein, J.R., Stamatakis, M.G., Dowling, J.S., 2000. Trace metal-rich Quaternary hydrothermal manganese oxide and barite deposit, Milos Island, Greece. Trans. Inst. Min. Metall., B 109, B67–B76.

Hekinian, R., Hoffert, M., Larqué, P., Cheminée, J.L., Stoffers, P., Bideau, D., 1993. Hydrothermal Fe and Si oxyhydroxide deposits from south Pacific intraplate volcanoes and East Pacific Rise axial and off-axial regions. Econ. Geol. 88, 2099–2121.

Juteau, M., Michard, A., Albarede, F., 1986. The Pb–Sr–Nd isotope geochemistry of some recent circum-Mediterranean granites. Contrib. Mineral. Petrol. 92, 331–340.

Kamenov, G.D., Mueller, P.A., Perfit, M.R., 2004. Optimization of mixed Pb–Tl solutions for high precision isotopic analyses by MC-ICP-MS. J. Anal. At. Spectrom. 19, 1262–1267.

Kamenov, G.D., Perfit, M.R., Jonasson, I.R., Mueller, P.A., 2005. High-precision Pb isotope measurements reveal magma recharge as a mechanism for ore deposit formation: examples from Lihir Island and Conical Seamount, Papua New Guinea. Chem. Geol. 219, 131–148.

Marani, M.P., Gamberi, F., Savelli, C., 1997. Shallow-water polymetallic sulfide deposits in the Aeolian Island Arc. Geology 25, 815–818.

Marani, M., Gamberi, F., Casoni, L., Carrara, G., Landuzzi, V., Musacchio, M., Penitenti, D., Rossi, L., Trua, T., 1999. New rock and hydrothermal samples from the southern Tyrrhenian Sea: the MAR-98 research cruise. G. Geol. 61, 3–24.

Marani, M.P., Gamberi, F., Bonatti, E. (Eds.), 2004. From Seafloor to Deep Mantle: Architecture of the Tyrrhenian Backarc Basin. Mem. Descr. Carta Geol. Ital., vol. 64, p. 196.

Marchig, V., Gundlach, H., Möller, P., Schley, F., 1982. Some geochemical indicators for discrimination between diagenetic and hydrothermal metalliferous sediments. Mar. Geol. 50, 241–256.

Michard, A., 1989. Rare earth element systematics in hydrothermal fluids. Geochim. Cosmochim. Acta 53, 745–750.

Olivarez, A.M., Owen, R.M., 1989. REE/Fe variations in hydrothermal sediments: implications for the REE content of seawater. Geochim. Cosmochim. Acta 53, 757–762.

Pichler, T., Veizer, J., 1999. Precipitation of Fe(III) oxyhydroxide deposits from shallow-water hydrothermal fluids in Tutum Bay, Ambitle Island, Papua New Guinea. Chem. Geol. 162, 15–31.

Puchelt, H., 1973. Recent iron sediment formation at the Kameni Islands, Santorini (Greece). In: Amstutz, G.C., Bernard, A.J. (Eds.), Ores in Sediments. Springer, Berlin, pp. 227–245.

Puchelt, H., Schrock, H.H., Schroll, E., 1973. Rezente marine Eisenerze auf Santorini Griechenland: I. Geochemie, Entstehung, Mineralogie. Geol. Rundsch. 62, 786–803.

Reyss, J.L., Lemaiter, N., Ku, T.L., Marchig, V., Southon, J.R., Nelson, D.E., Vogel, J.S., 1985. Growth of a manganese nodule from Peru Basin: a radiochemical anatomy. Geochim. Cosmochim. Acta 49, 2401–2408.

Rozanova, T.V., Gorshkov, A.I., Gorodnickiy, A.M., 1988. Mineral composition of iron ochres from the Marsili Seamount (Tyrrhenian Sea). Proceedings of the 8th Conference on Marine Geology, Gelendjik 4, 177–178.

Savelli, C., Gasparotto, G., 1994. Calcalkaline magmatism and rifting of the deep-water volcano of Marsili (Aeolian back-arc, Tyrrhenian Sea). Mar. Geol. 119, 137–147.

Sborshchikov, I.M., Savelli, C., Puchelt, H., Pescatore, T., Schreider, A.A., Yastrebov, V.S., 1988. Some volcano-tectonic features of Marsili Seamount (Tyrrhenian Sea): first report of two submersible dives. XXXI Congress-Assemble Plenier de la C.I.E.S.M. (Athens 17–22 October 1988), Abstract, p. 1.

Schwertmann, U., Fischer, R.W., 1973. Natural "amorphous" ferric hydroxide. Geoderma 10, 237–247.

Shotyk, W., Weiss, D., Appleby, P.G., Cheburkin, A.K., Frei, R., Gloor, M., Kramers, J.D., Reese, S., Van Der Knaap, W., 1998. History of atmospheric lead deposition since 12,370 ^{14}C yr BP from a Peat Bog, Jura Mountains, Switzerland. Science 281, 1635–1640.

Sedwick, P.N., McMurtry, G.M., Macdougall, J.D., 1992. Chemistry of hydrothermal solutions from Pele's vents, Loihi Seamount, Hawaii. Geochim. Cosmochim. Acta 56, 3643–3667.

Sun, S.-S., McDonough, W.F., 1989. Chemical and isotopic systematics of oceanic basalts: implications for mantle composition and processes. In: Saunders, A.D., Norry, M.J. (Eds.), Spec. Publ.-Geol. Soc. Lond., vol. 42, pp. 313–345.

Tommasini, S., Davies, G.R., Elliott, T., 2000. Lead isotope composition of tree rings as bio-geochemical tracers of heavy metal pollution: a reconnaissance study from Firenze, Italy. Appl. Geochem. 15, 891–900.

Uchupi, E., Ballard, R.D., 1989. Evidence of hydrothermal activity on Marsili Seamount, Tyrrhenian Basin. Deep-Sea Res. 36, 1443–1448.

Varnavas, S.P., Cronan, D.S., 1988. Arsenic, antimony and bismuth in sediments and waters from the Santorini hydrothermal field, Greece. Chem. Geol. 67, 295–305.